Journal of Archaeological Science: Reports 20 (2018) 748–755

Contents lists available at ScienceDirect

Journal of Archaeological Science: Reports

journal homepage: www.elsevier.com/locate/jasrep

A multi-technique investigation of the incuse coinage of Magna Graecia

F. Salvemini[a,*], K. Sheedy[b], S.R. Olsen[a], M. Avdeev[a], J. Davis[a], V. Luzin[a]

[a] Australian Nuclear Science and Technology Organisation, Lucas Heights, NSW 2234, Australia
[b] Australian Centre for Ancient Numismatic Studies, Macquarie University, Macquarie, NSW 2109, Australia

ARTICLE INFO

Keywords:
Archaeometallurgy
Neutron tomography
Neutron diffraction
Neutron texture
Non-invasive method
Numismatic materials
Ancient minting technology
Incuse coins

ABSTRACT

This paper focuses on the application of different neutron techniques to characterize the manufacturing process of 'incuse' coins minted by Greek colonies in Southern Italy during the 6th and 5th centuries BC. In order to provide an insight into incuse coinage minting, numismatic and historical studies were combined with metallurgical research based on non-destructive neutron diffraction, neutron texture analysis and neutron tomography. The most significant scientific data collected during our campaign of investigation will be showcased.

1. Introduction

The manufacturing technique of one of the earliest coinages in the world, the incuse coinage of the Greek colonies in South Italy, is poorly understood (Gorini, 1975; Rutter, 2001; Scavino, 2011; Williams, 1983). We know from archaeological evidence that in the mid- 6th century BC the city states of Sybaris (Fig. 1a) and Metapontum (Fig. 1b) began to mint a very distinct form of silver coin whereby the image struck in relief on the obverse is repeated on the reverse but incuse or intaglio – hence the name 'incuse coins'. Incuse coins, all struck on the same unique Achaean weight standard (with a stater of *c.*8.1 g; cf. Rutter, 2001: 4) were subsequently produced by other important cities, notably Croton, Caulonia and Poseidonia, and by a series of small mints associated with Sybaris (such as Sirinos and Pyxoes). Incuse coins were also minted by cities in other part of South Italy, though in lesser quantities. The Laconian colony of Taras (Rutter, 2001: 52–57) began minting a brief series of incuse coins around 520 BCE, as did Rhegium and Zancle (Rutter, 2001: 108–110), cities on the straits of Messina.

The reasons for the adoption of the incuse technique for minting coins, and indeed the actual processes involved in producing these coins (the preparation of the flan, the method of applying the dies) have been the subject of on-going discussion, though with relatively little application of scientific analysis (Williams, 1983; Elam, 1931; Giovannelli et al., 2005).

In this paper we report on a joint research project initiated by the ACANS (Australian Centre for Ancient Numismatic Studies) and ANSTO (Australian Nuclear Science and Technology Organisation) which aims to provide an explanation for the techniques of minting incuse coinage by combining numismatic and historical studies with metallurgical research based on neutron diffraction, neutron texture analysis and neutron tomography.

2. Neutron radiation methods in numismatics

NeuNtron radiation techniques are a relatively well-known and important means in archaeology for the non-invasive investigation of heritage materials (Kockelmann et al., 2004; Artioli, 2007; Lehmann, 2010). Compared to other sub-atomic particles, i.e. electrons or protons, neutrons are uncharged; they can penetrate deeply into matter and interact with the nucleus of an atom rather than with the diffuse electron cloud. These fundamental properties make neutron radiation techniques the ideal means to survey the bulk of dense materials such as metals (Furrer et al., 2009).

Neutron imaging has proven to be a valuable scientific analytical tool in archaeometric studies. It is a means to extract and quantify information on topics such as morphology, porosity, and inclusions. It detects the presence of composite structures with acceptable resolution and accuracy. Most importantly, it is non-destructive (Lehmann, 2010). Relevant information on the manufacturing process and the state of conservation can be inferred from the characterization and evaluation of internal structural features (Salvemini et al., 2016).

In applications to numismatics, Adriaens et al. (2010) used neutron tomography to supplement the X-ray diffraction (XRD) analysis of three coins from Israel (c. 6th–9th century AD). This allowed a reading of the

* Corresponding author.
E-mail address: filomena.salvemini@ansto.gov.au (F. Salvemini).

https://doi.org/10.1016/j.jasrep.2018.06.025
Received 27 February 2018; Received in revised form 21 May 2018; Accepted 14 June 2018
Available online 26 June 2018
2352-409X/

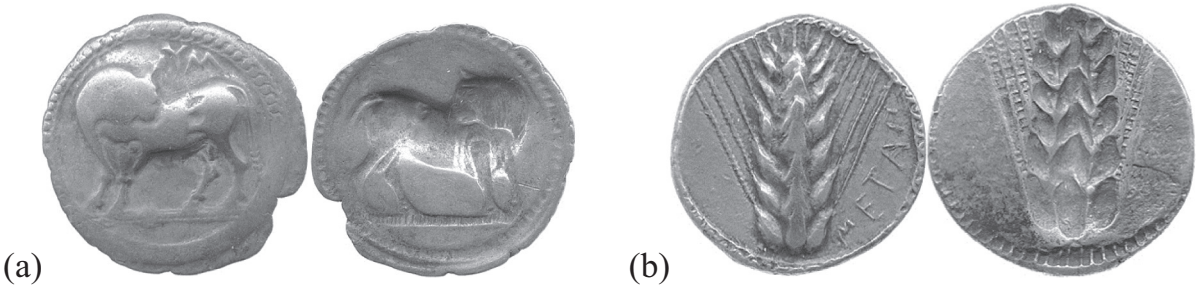

Fig. 1. Incuse stater, ACANS 730 (Sybaris c. 550–510 BCE, 7.73 g) and ACANS 526 (Metapontum c.540–510 BCE, 7.98).

coin inscriptions, where preserved, beneath the layers of corrosion. Similarly, Nguyen (2011) applied neutron tomography to analyse and identify heavily corroded coins. Neutron tomography was used by Contentgriesser et al. (2012) to gain information on the casting technique employed to produce highly leaded ancient bronze coins. More recently, Herringer et al. (2018), were able to clarify the casting process of a set of Roman brass sestertii with the help of neutron tomography.

While neutron imaging can disclose the inner structure and morphology, neutron diffraction can provide qualitative and quantitative data about 1) phase composition; 2) crystal and magnetic structures of each constituent phase; 3) (residual) microstrains and macrostrains; and 4) crystallographic texture (Kockelmann et al., 2006; Liang et al., 2009).

Neutron diffraction full pattern analysis is a relatively standard technique for the analysis of objects in cultural heritage studies (Rinaldi et al., 2002). Kirfel et al. (2011) used neutron diffraction full pattern analysis to study ten Southern Arabian coins (c. 4th–3rd centuries BC). Apart from the characterization of the phase composition (Ag vs Cu) they were able to distinguish between flans that had been cast, and those that had been free-poured and struck. Siouris et al. (2012) also employed full neutron diffraction profile analysis to characterize phase composition in ten silver-copper Thracian coins of the 5th century BC, including some plated coins. Canovaro et al. (2013) studied 12 bronze coins to determine the amount of tin in the bronze through full neutron diffraction pattern analysis. Corsi et al. (2016) used neutron diffraction analysis on a group of 30 coins from varying Celtic settlements in Northern Italy from the 5th–4th centuries BCE to correlate the time frame and probable minting history through the measurement of the silver-copper content; here they were able to demonstrate a general debasement in silver content from > 95% to around 70% over three centuries.

Neutron diffraction texture (or crystal preferred orientation) analysis is a highly appropriate means to investigate questions regarding the technology of production for cultural heritage objects (Artioli, 2007). The application of neutron diffraction texture analysis to numismatics, however, is relatively uncommon. Xie et al. (2004) used neutron diffraction for the comparative analysis of two Thracian bronze coins (c.450–350 BCE) in an attempt to assess their authenticity. The experimentally determined crystallographic texture, which showed axial compression for both, suggested the same (physically) production process (i.e. the metal flan was struck between two dies). Kockelmann et al. (2006) published texture analyses of six silver Thalers from the 16th century which confirmed the historically documented evolution of the Thaler fabrication technique (from hammer striking to the machine minting of coins from rolled metal sheets). Neutron texture analysis was extended into experimental archaeometry by Siano et al. (2006) with the texture measurement of a series of test pieces produced in controlled conditions and compared to the texture measurements of a Roman bronze coin.

A neutron radiation study may be complemented by the determination of the elemental composition of the coins. The composition can provide useful information regarding the manufacturing technology, age, minting places, and authenticity of the sample. The current analytical study of the incuse coins is still ongoing; data concerning elemental composition are not presented in the current work and relevant results will be disclosed in future publications.

3. Materials

In this paper we wish to outline in general terms our techniques of analysis and to consider preliminary results. A full report will be presented in forthcoming publications. The focus of the study was a group of incuse coins from the ancient localities of Metapontum, Kroton, Sirinos/Pyxoes, Sybaris, Caulonia and Taras in South Italy which may all be dated between 550 BCE and 470 BCE (Salvemini et al., 2016; Sheedy et al., 2015). This set of samples mostly came from the Gale Collection at the Australian Centre for Ancient Numismatic Studies (ACANS), one of the most important collections of ancient South Italian coins in the world (Sheedy, 2008). For comparative study, samples of non-incuse coins with better documented manufacturing techniques, from the same or later periods and different regions (i.e. a silver English penny from the reign of Edward I minted in 1270 CE) were also characterized (Table 1).

Table 1
ACANS silver incuse (Metapontum, Sybaris, Croton, Taras) and non-incuse (Aegina, Corinth, Athens, England) coins studied.

ACANS catalogue numbers:	Mint Date	Diameter (mm)	Thickness (mm)	Weight (gm)	Incuse	Mint
07GS526	c.510–470 BCE	22.7	1.9	7.94	Yes	Metapontum
07GS527	c.510–470 BCE	24.3	1.7	8.07	No	Metapontum
07GS513	c.540–510 BCE	26.5	1.4	8.14	Yes	Metapontum
07GS731	c.550–510 BCE	29.6	1.0	7.00	Yes	Sybaris
07GS1020	c.530–500 BCE	29.9	1.0	7.43	Yes	Croton
07GS181	c.550–500 BCE	23.8	1.7	7.76	Yes	Taras
03A73	c.530–525 BCE	Not circular	Uneven	12.07	No	Aegina
08A47	4th century BC	23.3	1.9	8.36	No	Corinth
01 M63	c.393–300 BCE	22.0	4.3	17.23	No	Athens
Private Collection	1270 CE	18.0	0.52	1.37	No	Edward I, England

Sample	Tomography	Texture		
	xy cross section	Ag(111)	Ag(200)	Ag(220)
1. ACANS 07GS526. **Metapontum** c. 510-470 BC AR Incuse stater. Ø 22.7 mm; th = 1.9 mm; M = 7.94 g 	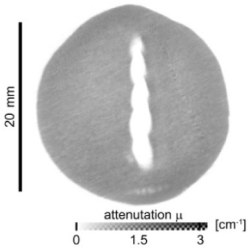	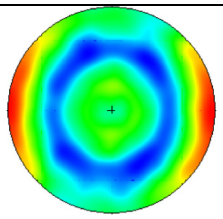 min: 0.77 max: 1.37	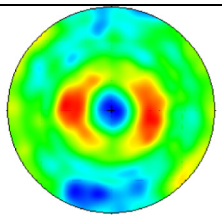 min: 0.83 max: 1.16	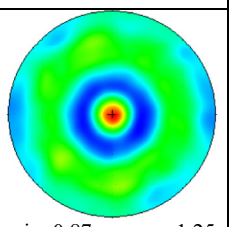 min: 0.87 max: 1.25
2. ACANS 07GS527. **Metapontum** c. 510-470 BC AR Incuse stater. Ø 24.3 mm; th = 1.7 mm; M = 8.07 g 	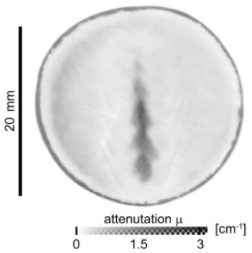	For this coin, the texture analysis consists of two sets of pole figures, one for the bronze core and another for the silver outer layer. It does not make sense to compare the texture of the bulk silver coins with the texture of a thin outer layer of the current coin (or the texture of the bronze core with texture of the other bulk silver coins), the dataset has been omitted from this sample.		
3. ACANS 07GS513. **Metapontum** c. 540-510 BC AR Incuse stater. Ø 26.5 mm; th = 1.4 mm; M = 8.14 g 	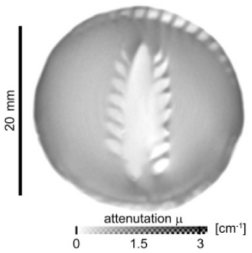	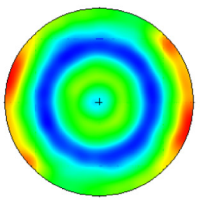 min: 0.72 max: 1.44	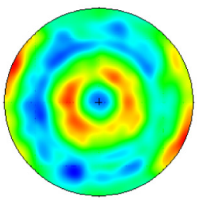 min: 0.84 max: 1.19	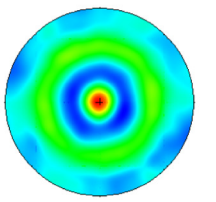 min: 0.82 max: 1.36
4. ACANS 07GS731 **Sybaris** c. 550-510 BC AR Incuse stater. Ø 29.6 mm; th = 1.0 mm; M = 7.00 g 	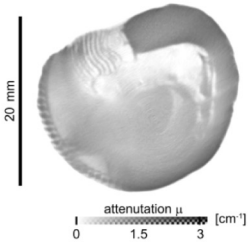	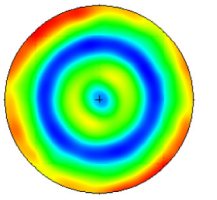 min: 0.58 max: 1.51	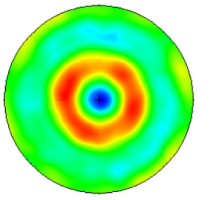 min: 0.67 max: 1.27	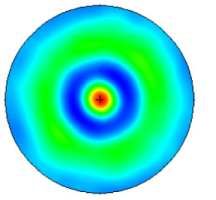 min: 0.68 max: 1.75
5. ACANS 07GS1020 **Croton** 530-500 BC AR Incuse stater Ø 29.9 mm, th = 1.0 mm, M=7.43g 	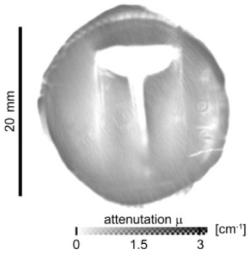	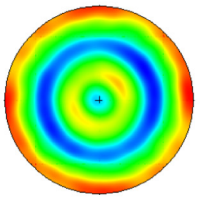 min: 0.57 max: 1.44	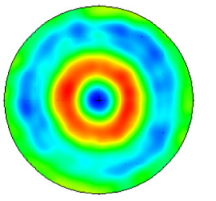 min: 0.77 max: 1.24	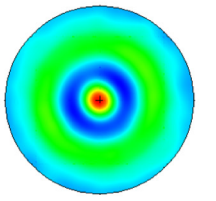 min: 0.69 max: 1.63
6. ACANS 07GS181. **Taras** c. 510-500 BC AR Incuse stater. Ø 23.8 mm; th = 1.7 mm; M = 7.76 g 	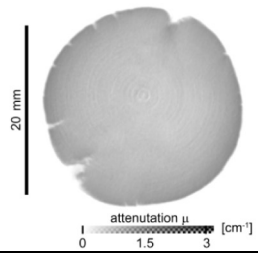	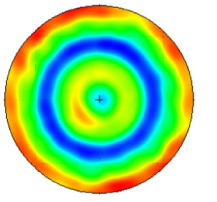 min: 0.76 max: 1.26	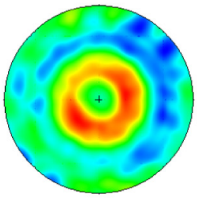 min: 0.82 max: 1.19	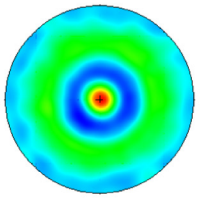 min: 0.82 max: 1.37

Fig. 2. From left to right: photographic image of the obverse and the reverse; xy-cross-section through the tomographic reconstruction; pole figures of the samples. The grey tone for the rendering of the neutron attenuation μ [cm^{-1}] is explicated by the scale at the bottom of each tomograph. In the chosen colouring scheme for pole figures, red corresponds to max pole figure density value while blue corresponds to min density value; the min and max values are given for each individual pole figure. (For interpretation of the references to colour in this figure legend, the reader is referred to the web version of this article.)

7. ACANS 03A73 **Aegina** c.530-525 BC AR Non-Incuse stater (Didrachm) Ø Irregular, max 23 mm; M = 12.07g. 	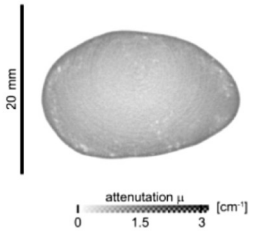 *see Figure 3, a for map of porosities	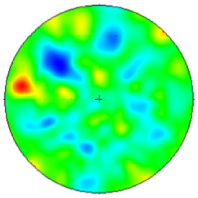 min: 0.47 max: 1.86	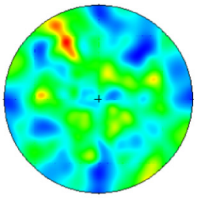 min: 0.54 max: 2.00	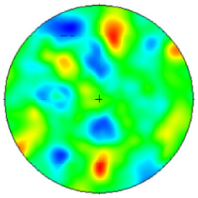 min: 0.59 max: 1.54
8. ACANS 08A47 **Corinth** 4th century BC AR Non-Incuse stater. Ø 23.3 mm; th = 1.9 mm; M = 8.36g. 	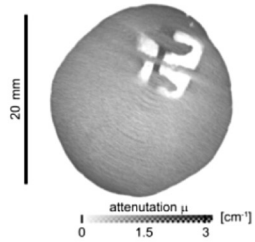	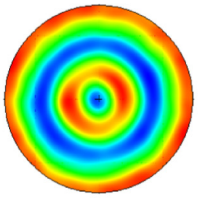 min: 0.49 max: 1.47	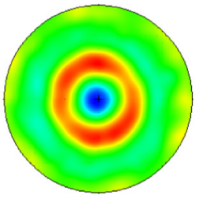 min: 0.47 max: 1.39	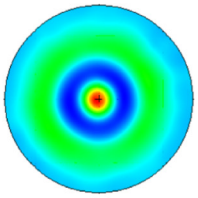 min: 0.53 max: 2.13
9. ACANS 01M63 **Athens** 393-300 BC Ø 22.0 mm; th = 4.3 mm; M = 17.23g. 	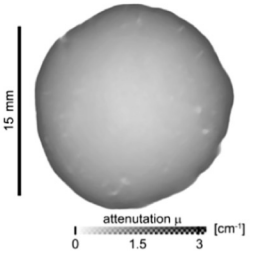 *see Figure 3, b for map of porosities	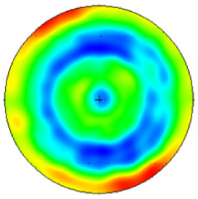 min: 0.80 max: 1.30	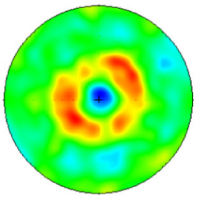 min: 0.80 max: 1.18	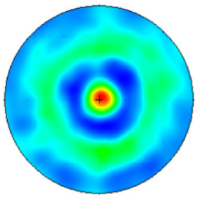 min: 0. 85 max: 1.44
10. Private Coll. **Edward I** 1270 AD. Silver penny. Ø 18 mm; th = 0.52 mm; M = 1.37g. 	* the tomographic analysis of this sample is not yet available.	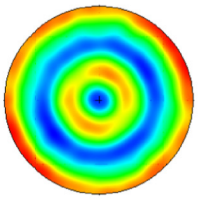 min: 0.60 max: 1.44	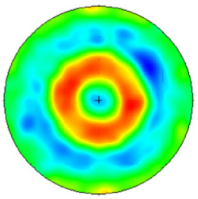 min: 0.73 max: 1.26	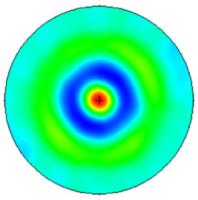 min: 0.65 max: 1.68

Fig. 2. (*continued*)

4. The neutron beam instrumentation and measurement procedures

The samples were characterized using three neutron beam instruments at ANSTO; the high resolution powder diffractometer ECHIDNA (Liss et al., 2006), the residual stress and texture diffractometer KOWARI (Kirstein et al., 2009), the radiography and tomography instrument DINGO (Garbe et al., 2015).

On DINGO, the high spatial resolution configuration (with the ratio of collimator-detector length L to inlet collimator diameter D equals to 1000), corresponding to a pixel size of 27 μm, was used to detect the smallest structural feature within the bulk of the coins. During the measurement, projections were obtained by rotating the sample around its vertical axis for 1339 angles equiangularly spaced from 0° to 360°. At each step the coins were exposed to the neutron beam for a period of 60s. The portion of the beam transmitted through the sample is converted into visible light using a 50 μm thick ^{6}LiF/ZnS scintillator, which is then guided via a mirror to an Andor DW434 CCD camera with 1024 × 1024 pixels. The size of the neutron beam available on the machine permits from three to four coins to be studied at one time by stacking the coins vertically, with a separation by 5–10 mm by thin aluminium foil (aluminium is nearly transparent to neutrons and does not appear in the tomographic images). The data sets were reconstructed with the Octopus package (Dierick et al., 2004), while AVISO 9.1 (FEI, n.d.) was used for visualization and analyses.

Complementary investigation by neutron diffraction analysis on the High Resolution Powder Diffractometer ECHIDNA was undertaken at 1.6 Å. The diffraction pattern was processed by using the GSAS code (Larson and Von Dreele, 2004) in order to perform Rietveld refinement of the diffractogram and extract crystallographic information including phase composition.

In the texture experiments, the sample was mounted onto a goniometer, and a diffraction pattern was measured by the neutron 2D position sensitive detector at each sample orientation covering approximately a 15° range (and size of the KOWARI detector). Overall, some 1200 individual sample orientations were measured; these correspond approximately to a 5° × 5° equi-angular grid on a hemisphere. The prime index pole figures of Ag (fcc metal) - Ag(111), Ag(200), Ag (220) and Ag(311) - were collected through the detection of the intensity of the diffraction peak of the corresponding (*hkl*) reflection.

Despite the high penetration ability of neutrons the very anisotropic shape of the coins impacts significantly on the quantitative texture analysis. Neutrons are attenuated differently in different orientations, depending on the specimen thickness, and exact shape. In some of the coins studied, the attenuation effect can reach a factor of > 20 (a ratio between diffraction peak intensities in the least and most attenuated

direction within the coin). Pole figure measurements constitute experimental detection of the same peak intensity as a function of the sample orientation. Therefore attenuation interferes and affects significantly the results of texture observations. This problem can usually be resolved by applying absorption corrections. These corrections can be calculated theoretically from the geometrical characteristics (shape, thickness and diameter) and attenuation properties of the coin material (Luzin and Brokmeier, 2002). Alternatively, these corrections can be found empirically through an analysis of self-consistency in the set of pole figures, which can be evaluated by means of the texture analysis. In short, if applied corrections are well determined, the pole figures recalculated through the ODF (Orientation Distribution Function) reconstruction analysis should match well the experimental (corrected) pole figures. If not the process of finding a smooth correction function can be repeated iteratively to achieve the best result in terms of the goodness-of-fit. The latter treatment was used and the corrected pole figures are reported in this work.

5. Results

The results of the tomographic and texture analyses in Fig. 2 display common macrostructural and microstructural features for the incuse coins samples 07GS513, 07GS731, 07GS1020, 07GS181. The virtual cross-sections through the tomographic reconstructions show a homogeneous bulk, free of any inclusions or macro-porosities. A coin minted in Corinth (08A47) shows a similar pattern. In contrast, the two non-incuse coins from Aegina and Athens display a porous structure (Fig. 3).

In support, the presence of the texture (110)-fiber component (Xie et al., 2004) is demonstrated (by the texture analysis) in all incuse coins. The degree of the preferred orientation is apparently different in the coins sampled and can be judged in the easiest way by comparing the minimum and maximum values of the Ag(220) pole figure since the (110)-fiber component – (110) and (220) are crystallographically equivalent (evident as the peak of intensity in the centre of the pole figure). To eliminate the effects related to some experimental statistical uncertainties, the Ag(220) pole figures were averaged over the azimuthal angle. In this way, all coins can be easily compared in terms of one dimensional pole density distribution with their minimum and maximum values (Fig. 4). Within our sample selection the strongest texture is exhibited by the Corinth coin (sample 08A47) with max ~2. The coin with almost no preferred orientation (density is 1 everywhere, random texture) is from Aegina (sample 03A73), though this very weak distribution is masked on pole figures by a visible “spottiness” due to the large grain microstructure. (In the pole figures the bright spots correspond to the large grains.) The data from all other selected coins fall between these two most extremes.

The analysis of the diffraction data from the ANSTO/ACANS program of neutron radiation studies is still in progress; however, some interesting preliminary results are here highlighted.

By comparing the neutron diffraction patterns of two incuse coins from Metapontum – 07GS526 07GS527 – the contrast is clear. Despite the two coins being very similar in appearance, the analysis of their diffraction patterns (Fig. 5) indicates that 07GS527 has a composite structure made of silver and copper. Corroborated by neutron tomography analysis (Salvemini et al., 2016), neutron diffraction allows the volume/mass of the constituent phases to be quantified with accuracy better than 1%. In the case of 07GS527, the fraction of silver, a 0.5 mm thick silver layer over the copper/bronze core, was estimated ~25% of the coin volume.

6. Discussion

The neutron tomographic reconstructions show a clear commonality in the internal macrostructure of the incuse coin samples (1–6). Here we see a bulk metal free of inclusions and voids. In general this is typical of metal that was subjected to a significant degree of working, e.g. forging or hammering. In fact, only subtle variations are detectable for the neutron attenuation coefficient ($2.5 \pm 0.25\,cm^{-1}$) expressed as a grey-tones scale in the tomographic cross-sections (Fig. 2). These are mostly artefacts (beam hardening and rings) that couldn't be completely filtered during the reconstruction process without compromising the quality of the image. Among the non-incuse coin samples investigated (7–10) a lack of features can be also observed in the Corinthian stater, sample 8 (ACANS inv.08A47). In contrast, the samples from Athens (sample 9) and Aegina (sample 7) show typical casting defects and porosity (Fig. 2). Porosity was also observed in two coins, an Athenian tetradrachm ACANS inv.14A07 and the Metapontum stater ACANS *SNG* 525, investigated during the first campaign of measurements (Salvemini et al., 2016).

In the casting process, the solubility of the gases dissolved in the liquid decreases as the molten metal cools down; once the solubility limit is reached, pores originate (Scott et al., 1994). Several variables can influence the amount, geometry, size, orientation, location and connectivity of pores. During casting, factors like the type of mould, the melt temperature, the solidification rate, the solubility and the internal pressure of the gas, can play a major role (Campbell, 2011). Afterwards, if the cast metal undergoes further work i.e. hammering, annealing, etc., these actions can modify the shape, and significantly reduce the

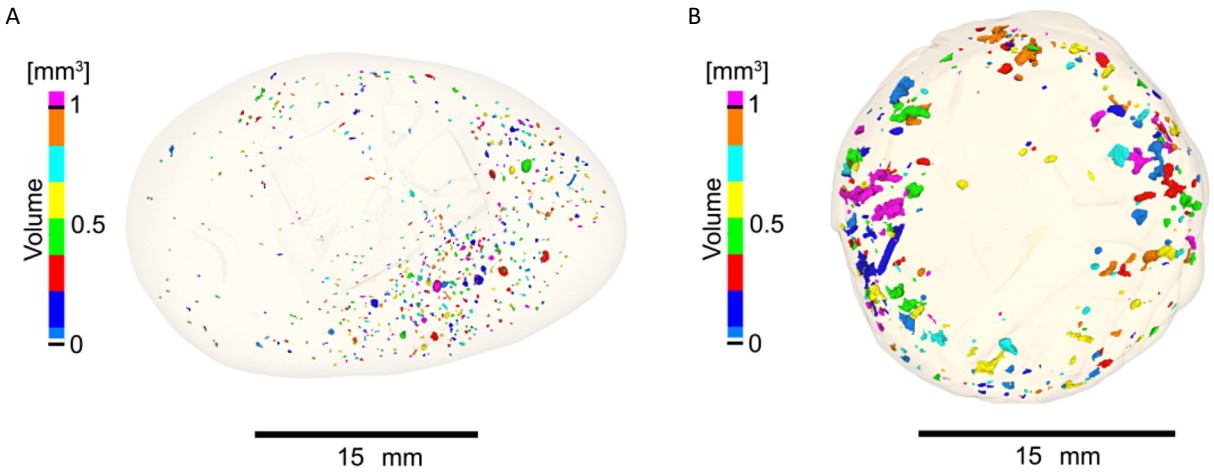

Fig. 3. Tridimensional map of porosities in a) the Aeginian sample 5 (ACANS 03A73) and b) Athenian coin 7 (ACANS 01M63). The colour code adopted to render the volume of the detected pores is indicated by the chart on the left side. (For interpretation of the references to colour in this figure legend, the reader is referred to the web version of this article.)

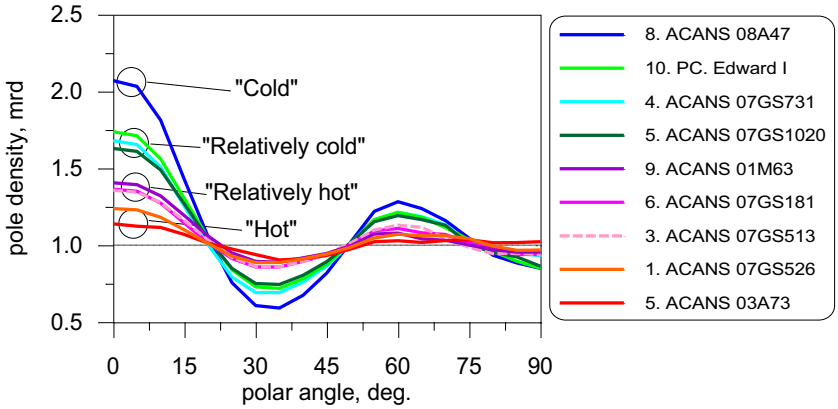

Fig. 4. Average Ag(220) pole figure density for the coins with different strengths of texture. Several groups are differentiated based on the average minimum/maximum values.

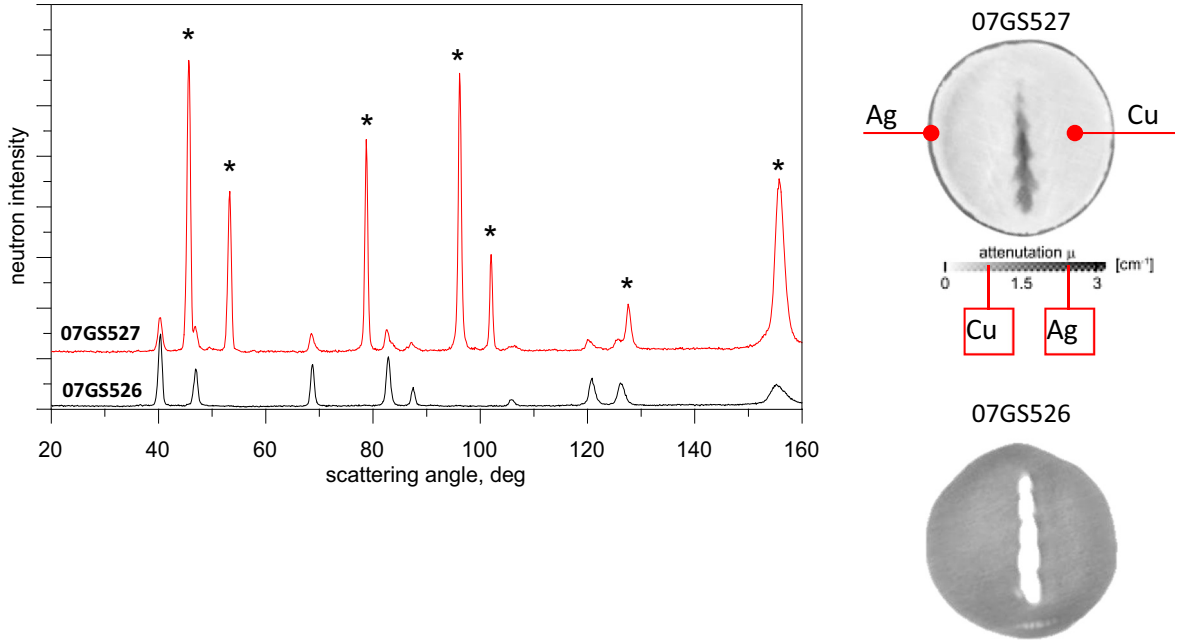

Fig. 5. On the left, neutron diffraction patterns for 07GS526 and 07GS527. The diffraction pattern of 07GS526 shows 'pure' silver, while that for 07GS527 reveals the presence of two phases (silver and copper/bronze); the additional diffraction peaks from copper/bronze in 07GS527 are indicated by the star symbol. On the right, xy-cross-sections through the tomographic reconstructions of the two samples are reported. A scale of the neutron attenuation coefficient is reported on the bottom right. The attenuation across the bulk of coin **07GS526** appears constant. The central empty area is due to the cropping plane intersecting the figurative type. The attenuation detected for the core material of 07GS527 clearly differs from the previous sample. On the other hand, the outer rim is highly attenuating confirming the application of a plating layer (Salvemini et al., 2016).

size or number of pores. The coins from Athens, Metapontum, and Aegina differ in amount, size and distribution of pores, thus suggesting the use of different casting conditions and/or method of refining the flan. However, in all samples, pores are more densely distributed around the figurative type. This can be related to the action of striking that probably caused the obliteration of pores in the portion of the bulk beneath the area of impact of the dies. A more in-depth statistical analysis on the distribution and size of the porosities will be reported and discussed in a dedicated publication.

It seems evident that in the production of incuse coins, the cast metal blank was subjected to working before being finally struck with the coin dies in a way similar to the Corinthian stater (sample 8). However the minting technique cannot be determined unambiguously from neutron tomographic reconstruction alone and we must look at the data from the neutron texture investigation for more decisive proof. All incuse coins studies in this project feature a very similar and well defined patterning of the (110)-fiber texture component (though with a certain variation in the strength of texture) which we suggest is the result of an extensive working of the metal. The variation in the strength of texture reflects natural differences in the amount of plastic deformation (hammering, annealing, and striking) applied to coins as well as the temperature of the flans during manufacturing.

Ideally, for full quantitative interpretation of the texture results, both deformation and temperature dependences (and possibly purity) of silver are to be known or studied, in the way similar to Siano et al. (2006) with a series of test "standards" deformed in controlled conditions. Based on our preliminary results for silver (a full study will be published elsewhere), the temperature dependence is the most critical factor for coin texture; the general rule is that cold working produces stronger texture during coin production. Our analysis of the temperature at production can be based on the measure of the texture strength. In particular, the analysis of the (110) pole figure and (110) component is the most prominent way. Without diminishing the value of theresults, but somehow simplifying the non-linear temperature dependence of the

texture strength, a relative scale of temperature is considered here with such temperature grades given as 'cold', 'relatively cold', 'relatively hot' and 'hot'. In the absolute scale, 'cold' corresponds to temperature of approximately 200 °C, while 'hot' corresponds to 700 °C or even above.

Two of the incuse coins, sample 4 (Sybaris) and sample 5 (Croton), show strong indications of cold working with a higher preferred orientation of the crystallites. Their pole figures resemble that of the hammered silver penny (sample 10), and one might conclude that there were similarities in the treatment of the metal (similar deformation-temperature conditions), even though the exact instrumentation of minting may (but not certainly) have been different. Sellwood has shown (Sellwood, 1962) that English pennies were made by beating a sheet of silver to about 0.5 mm and then cutting out a circular coin blank of the appropriate diameter before striking the coin between two dies.

Two other incuse coins, sample 3 (Metapontum) and sample 6 (Taras), demonstrate lower degrees of texture development that might be attributed to higher temperature or, possibly, to a lesser degree of plastic deformation induced by the minting process. These coins indicate rather hot working at temperature relatively close to the silver melting temperature (~960 °C).

These data sets are in good agreement with the observations by Giovannelli et al., 2005 conducted on a set of incuse coins from Metapontum and Caulonia (Giovannelli et al., 2005). Metallographic and SEM examination of the loose metallic remnants showed the presence of deformation twins and strain lines within the grains, which denote work-hardening on recrystallized flans as the striking process was presumably performed at ambient temperature. Large polygonal grains possessing concave boundaries were also observed, suggesting that secondary recrystallization has taken place. Therefore, the metal was subjected to annealing during fabrication.

The discussed evidence for the extensive treatment of the flans of the incuse coins prior to minting are supported by the contrasting pole figures observed in the archaic coin from Aegina, sample 7. The pole figures are without clear patterning and apparently have an almost random distribution of large grains. This is typical of metal that has not been worked but rather poured into a mould and then, when still hot, struck with dies to produce the coin. These pole figures with a "spotty" appearance indicate slow cooling after casting, with grain growth and the formation of dominant large grains (dendrites). The pole figures exhibit some very weak fiber texture that apparently comes from the last step of striking; this cannot be seen in the original pole figures, but can only be visualised when analysed statistically (Fig. 4).

In contrast, sample 8 from Corinth has the most extreme values in the pole figures. It should be noted that this coin was minted in the 4th century and is significantly later than the archaic issues (samples 1–7); this suggests a different method of minting. The non-incuse Athenian coin (sample 9), which is also from the 4th century BC, shows mixed signatures of metalworking. On one side we see that the texture is analogous to the hot-worked samples 3 and 6 (07GS513 and 07GS181), but on the other, it exhibits porosity that is more typical of cast metal. Given that the porosity is concentrated around the circumference of the coin, these two seemingly contradictory facts can be reconciled by assuming a lack of uniformity in the working of the metal that resulted in a high degree of deformation in the central part in contrast to a low degree of deformation in the outer parts of the coin.

One manufacturing technique was clearly identified: plating. The neutron tomographic reconstruction of sample 2, a stater from Metapontum (07GS527), identified the presence of a core made of a low attenuating material, wrapped by a highly attenuating layer. In accordance with the phase analysis of the neutron diffraction pattern, a copper-based alloy was used as core and silver sheet for the plating (Salvemini et al., 2016).

7. Conclusion

Neutron tomography, phase and texture analyses were applied in this study to investigate differences and similarity between coins produced with the earliest minting methods of the ancient Greek world. Using these techniques of analysis we have characterized the internal macrostructure, the composition and the degree of the preferred orientation on a selection of samples. Data from the incuse staters were cross-correlated to those collected from coins of better documented manufacturing techniques, from previous or later periods and different regions which were used as references.

The evidence for the extensive treatment of the cast flans prior to minting was supported by the concordant tomographic and pole figure results observed for the incuse coins. In contrast to the archaic coins from other centres such as Aegina and Athens (but resembling the later Corinthian stater and English penny) the silver flans of the incuse coins were very likely hammered and annealed, though to different degrees, and we take this to be a salient feature of coin production in the Greek colonies in South Italy.

Incuse coin production in general requires a high level of technical competency. As highlighted by our neutron diffraction and imaging results, the practice of plating was known in these South Italian mints. Here we wish to point out that the plating of the extremely thin flans used for incuse coinage would have required a very high level of skill.

References

Adriaens, A., Dowsett, M., Lehmann, A., Farhi, J., Gunneweg, J., Bouchenoire, L., 2010. The coin beneath the crust: a pilot study of coins from the Mediterranean coast of Israel. In: Gunneweg, J., Adriaens, A. (Eds.), A Holistic View on Qumran and the Dead Sea Scrolls. Leiden.

Artioli, G., 2007. Crystallographic texture analysis of archaeological metals: interpretation of manufacturing techniques. Appl. Phys. A 89, 899–908.

Campbell, J., 2011. Complete Casting Handbook: Metal Casting Processes, Metallurgy, Techniques and Design. Elsevier.

Canovaro, C., Calliari, I., Asolati, F., Grazzi, F., Scherillo, A., 2013. Characterization of bronze Roman coins of the fifth century called Nummi through different analytical techniques. Appl. Phys. A 113 (4), 1019–1028.

Contentgriesser, M., Traum, R., Vondrovec, K., Vontobel, K., Lehmann, E., 2012. Application of X-ray and neutron tomography to study antique Greek bronze coins with a high lead. In: International Conference on the Use of X-ray (and Related) Techniques in Arts and Cultural Heritage (XTACH 11).

Corsi, J., Grazzi, F., Lo Giudice, A., Re, A., Scherillo, A., Angelici, D., Allegretti, S., Barello, F., 2016. Compositional and microstructural characterization of Celtic silver coins from northern Italy using neutron diffraction analysis. Microchem. J. 126, 501–508.

Dierick, M., Masschaele, B., Van Hoorebeke, L., 2004. Octopus, a fast and user-friendly tomographic reconstruction package developed in LabView. Meas. Sci. Technol. 15 (7), 1366–1370.

Elam, C., 1931. An investigation of the microstructures of fifteen silver Greek coins (500–300 B.C.) and some forgeries. J. Inst. Met. 45, 57–69.

FEI Online. Available: https://www.fei.com/software/amira-avizo/.

Furrer, A., Mesot, J., Strässle, T., 2009. Neutron scattering in condensed matter. Physics 4, 1–23.

Garbe, U., Randall, T., Hughes, C., Davidson, G., Pangelis, S., Kennedy, S., 2015. A New Neutron Radiography/Tomography/Imaging Station DINGO at OPAL. 10 World Conference on Neutron Radiography 5–10 October 2014.

Giovannelli, G., Natali, S., Bozzini, B., Sicilia, A., 2005. Microstructural characterization of Early Western Greek incuse coins. Archaeometry 47, 817–833.

Gorini, G., 1975. La monetazione incusa della Magna Grecia, Milano.

Herringer, S., Ryzewski, K., Bilheux, H., Bilheux, J., 2018. Evaluation of segregation in Roman sestertium coins. J. Mater. Sci. 53, 2161–2170.

Kirfel, A., Kockelmann, W., Yule, P., 2011. Non-destructive chemical analysis of old South Arabian coins, fourth century BCE to third century CE. Archaeometry 53, 930–949.

Kirstein, O., Luzin, V., Garbe, U., 2009. The strain-scanning diffractometer Kowari. Neutron News 20 (4), 34–36.

Kockelmann, W., Kirfel, A., Siano, S., Fros, C.D., 2004. Illuminating the past: the neutron as a tool in archaeology. Phys. Educ. 39 (2), 155–165.

Kockelmann, W., Siano, S., Bartoli, L., Visser, D., Hallebeek, P., Traum, R., Linke, M., Schreiner, Kirfel, A., 2006. Applications of TOF neutron diffraction in archaeometry. Appl. Phys. A 83 (2), 175–182.

Larson, A., Von Dreele, R., 2004. General Structure Analysis System (GSAS). Los Alamos National Laboratory Report.

Lehmann, E., 2010. Neutron tomography as a valuable tool for the non-destructive analysis of historical bronze sculpture. Archaeometry 52 (2).

Liang, L., Rinaldi, R., Schober, H., 2009. Neutron applications in earth, energy and environmental sciences. N. Y. 1, 1–13.

Liss, K.-D., Hunter, B., Hagen, M., Noakes, T., Kennedy, S., 2006. Echidna—the new high-resolution powder diffractometer being built at OPAL. Phys. B Condens. Matter 385–386 (Part 2), 1010–1012.
Luzin, V., Brokmeier, H.G., 2002. Attenuation corrections in neutron texture experiment. Mater. Sci. Forum 408-412, 191–196.
Nguyen, H.-Y., 2011. Computed Tomography for the non-destructive Imaging of Cultural Heritage: X-ray, Gamma and Neutron Sources, Kingston, Ontario (A thesis submitted to the Department of Art In conformity with the requirements for The degree of Master of Art Conservation Queen's University). .
Rinaldi, R., Artioli, G., Kockelmann, W., Kirfel, A., Siano, S., 2002. The contribution of neutron scattering to cultural heritage research. Notiziario neutroni e luce di sincrotrone 7, 30–37.
Rutter, N., 2001. Historia Numorum. Italy, London.
Salvemini, F., Olsen, S., Luzin, V., Garbe, U., 2016. Neutron tomographic analysis: material characterization of silver and electrum coins from the 6th and 5th centuries BC. Mater. Charact. 118, 175–185.
Scavino, R., 2011. Monetzione Incusa Magnogreca: destinazione e funzioni. The XIVth International Numismatic Congress, Glasgow.
Scott, D.A., Podany, J., Considine, B.B., 1994. Ancient & Historic Metals: Conservation and Scientific Research. Symposium on Ancient and Historic Metals Organized by the J. Paul Getty Museum and the Getty Conservation Institute, November 1991, Los Angeles.
Sellwood, D., 1962. Medieval minting techniques. Br. Numis. J. 31, 57–65.
Sheedy, K., Munroe, P., Salvemini, F., Luzin, V., Garbe, U., 2015. An incuse stater from the series 'Sirinos/Pyxoes'. J. Numis. Assoc. Aust. 26, 36–52.
Sheedy, K.A., 2008. Sylloge Nummorum Graecorum Australia I. The Gale Collection of South Italian Coins. Numismatic Association of Australia, Adelaide.
Siano, S., Bartoli, L., Santisteban, J.R., Kockelmann, W., Daymond, M., Miccio, M., De Marinis, G., 2006. Non-destructive investigation of bronze artifacts from the Marches National Museum of Archaeology using neutron diffraction. Archaeometry 48 (1), 77–96.
Siouris, I., Katsavounis, S., Kockelmann, W., 2012. Characterization of ancient Greek coins using non-destructive TOF neutron diffraction, 5th European Conference on Neutron Scattering. J. Phys. Conf. Ser. 340 (012112).
Williams, R.J., 1983. The Incuse Staters of Kroton. Ph.d thesis. Monash University.
Xie, Y., Lutterotti, L., Wenk, H.R., 2004. Texture analysis of ancient coins with TOF neutron diffraction. J. Mater. Sci. 39 (10), 3329–3337.